DESIGN OF INDUCTORS IN ELECTROMAGNETIC CASTING USING LEVEL-SETS AND SECOND ORDER TOPOLOGICAL DERIVATIVES

A. CANELAS, A.A. NOVOTNY, AND J.R. ROCHE

Abstract. We propose a new iterative method for the topology design of the inductors in electromagnetic casting. The method is based on a level-set representation of the solution together with first and second order topological derivatives. The optimal design is found by minimizing a Kohn-Vogelius functional for the problem. The complete topological expansion of the objective functional, which is herein given, is used to define the iterative step. Results for several numerical examples show that the technique proposed can be efficiently used in the design of suitable inductors.

1. Introduction

The design problem in electromagnetic casting is the determination of the electrical currents that shape certain mass of liquid metal into a predefined geometry, the target shape. In previous papers we studied this problem considering inductors made of single small solid-core wires [1], and large inductors made of bundled insulated strands [2]. In both cases the number of inductors was fixed in advance. In a recent paper we overcome this constraint, and looked for configurations of inductors considering different topologies with the purpose of obtaining inductors with more realistic geometric configurations [3].

In the present paper we formulate the design problem as an optimization problem by means of a shape functional based on the Kohn–Vogelius criterion [4, 5, 6, 7, 8]. The main achievements of the present paper are the following: First, we give the analytical expression of the complete topological asymptotic expansion of the Kohn–Vogelius shape functional, generalizing the results of [3] and proving that the expansion has actually a finite number of terms. Second, we use this topological asymptotic expansion to devise an efficient topology optimization algorithm based on the level-set technique proposed by Amstutz & Andrä [9]. The novelty of this paper is that we propose a topology optimization algorithm using non-standard level set method together with first and second order topological derivatives.

The contents of this paper are organized as following. Section 2 describes the direct free-surface problem concerning the electromagnetic casting and formulates the problem of designing suitable inductors as a problem of minimization of a Kohn–Vogelius-type objective functional. Section 3 introduces the topological derivative concept and states the asymptotic expansion of the Kohn–Vogelius functional. The numerical method is presented in Section 4. Some examples are presented in Section 5, to show that the method proposed can efficiently find suitable designs. The conclusions of this paper are presented in Section 6.

2. The electromagnetic casting problem

The electromagnetic casting is an industrial technique used in the preparation of very pure samples, preparation of aluminum ingots using soft-contact confinement of the liquid metal, shaping of components of aeronautical engines made of superalloy materials (Ni, Ti, ...), etc. [10, 11].

In this paper we study a vertical column of liquid metal falling down into an electromagnetic field created by vertical inductors. We assume that a stationary horizontal section is reached, so that the two-dimensional model is valid, and that the frequency of the imposed current is very

Key words and phrases. Topological asymptotic analysis, topological derivatives, inverse problem, electromagnetic casting.

high, so that the magnetic field does not penetrate into the metal (skin effect); see [12, 13, 14, 15, 16, 17, 18, 19].

The exterior boundary value problem regarding the magnetic field in terms of the flux function $\varphi : \Omega \to \mathbb{R}$ is:

$$\left\{ \begin{array}{rll} -\Delta\varphi & = \mu_0 j_0 & \text{in } \Omega\,, \\ \varphi & = 0 & \text{on } \Gamma\,, \\ \varphi(x) & = c + o(1) & \text{as } \|x\| \to \infty\,, \end{array} \right. \tag{2.1}$$

where $\Omega \subset \mathbb{R}^2$ is the exterior of the compact, simply connected and with a non-void interior, domain ω occupied by the cross-section of the metal column. In (2.1) Γ is the boundary of Ω, that we assume is at least of class C^2. By $\|\cdot\|$ we denote the Euclidean norm, the little-o notation means $\lim_{\|x\|\to\infty} o(f(x))/f(x) = 0$, $c \in \mathbb{R}$ is the value at infinity of the solution φ, which is also an unknown of (2.1) [1, 2, 3], μ_0 is the vacuum permeability, and j_0 is the vertical component of the electric current density vector, which is assumed compactly supported in Ω and such that the total current is zero:

$$\int_\Omega j_0 \, dx = 0\,, \tag{2.2}$$

Problem (2.1) has unique solutions $\varphi \in W_0^1(\Omega)$ and $c \in \mathbb{R}$ [20, 21], where $W_0^1(\Omega)$ is defined as:

$$W_0^1(\Omega) = \{u :\ \rho\, u \in L^2(\Omega) \text{ and } \nabla u \in L^2(\Omega)\}\,, \tag{2.3}$$

with $\rho(x) = [\sqrt{1+\|x\|^2}\,\log(2+\|x\|^2)]^{-1}$. The equilibrium of the liquid metal boundary is given by [18, 22, 23, 24, 25]:

$$\frac{1}{2\mu_0}\left|\frac{\partial\varphi}{\partial n}\right|^2 + \sigma\mathcal{C} = p_0 \quad \text{on } \Gamma\,, \tag{2.4}$$

where n is the outward-pointing unit normal vector of Γ, $\mathcal{C}$ is the curvature of Γ seen from the metal, σ is the surface tension of the liquid and the constant p_0 is an unknown of the problem. Physically, p_0 represents the difference between the internal and external pressures.

In the free-surface problem of electromagnetic casting the electric current density j_0 is given, and one needs to find the shape ω, having a given area $S_0 = \int_\omega dx$, such that the flux φ, solution to (2.1), also satisfies the equilibrium (2.4) for some real constant p_0.

2.1. **The design problem.** In the design problem we have to determine the current density j_0 satisfying (2.2) such that the solution φ of (2.1) also satisfies the equilibrium (2.4). It is known that at the equilibrium $p_0 = \max_\Gamma \sigma\mathcal{C}$ [15, 26, 3]. Therefore, for a given target shape with bounded curvature, p_0 can be calculated. Defining $\bar{p} = \sqrt{2\mu_0(p_0 - \sigma\mathcal{C})}$, the equilibrium equation in terms of the flux function reads

$$\frac{\partial\varphi}{\partial n} = \varkappa\,\bar{p} \quad \text{on } \Gamma\,, \tag{2.5}$$

where $\varkappa = \pm 1$, has the changes of sign located at points where the curvature of Γ is a global maximum. The two possible ways of defining $\varkappa$ lead to the same solution j_0 but with the opposite sign [3]. From (2.5) we have that a necessary condition for the existence of a solution is the following [3]:

$$\int_\Gamma \varkappa\,\bar{p}\, ds = 0\,. \tag{2.6}$$

It is known that the design problem is inherently ill posed: small variation of the liquid boundary may cause dramatic variations in the solution j_0 [15, 26]. In addition, the uniqueness of the solution in terms of j_0 cannot be ensured [15, 3]. Therefore, we formulate the design

problem as an optimization problem, looking for a solution (maybe just an approximate solution) that minimizes the following shape functional based on the Kohn–Vogelius criterion:

$$\psi(0) = J(\phi) = \frac{1}{2}\|\phi\|^2_{L^2(\Gamma)} = \frac{1}{2}\int_\Gamma \phi^2\, ds\,, \tag{2.7}$$

where the auxiliary function $\phi \in W^1_0(\Omega)$ depends implicitly on j_0 and c by solving the following boundary-value problem

$$\left\{\begin{array}{rll} -\Delta\phi & = \mu_0 j_0 & \text{in } \Omega\,, \\ \dfrac{\partial\phi}{\partial n} & = \varkappa\,\bar{p} - d(j_0) & \text{on } \Gamma\,, \\ \phi(x) & = c + o(1) & \text{as } \|x\| \to \infty\,, \end{array}\right. \tag{2.8}$$

where, denoting $|\Gamma| = \int_\Gamma ds$, $d(j_0)$ is defined as

$$d(j_0) = |\Gamma|^{-1}\int_\Omega \mu_0 j_0\, dx\,. \tag{2.9}$$

The term $d(j_0)$ is introduced in (2.8) to correctly define ϕ for j_0 not necessarily satisfying condition (2.2). In fact, given some fixed value c, and assuming that (2.6) is satisfied, problem (2.8) has a unique solution in $W^1_0(\Omega)$, see [21, 27].

In this paper we assume that condition (2.6) is satisfied, and look for j_0 satisfying (2.2) and a constant c such that the solution ϕ to (2.8) minimizes the shape functional (2.7). Note that the minimum is attained if $\phi \equiv 0$ on Γ. In this case, from the well-posedness of problems (2.1) and (2.8), we have $\phi \equiv \varphi$ in Ω. We can easily eliminate the variable c of the optimization problem by defining it as the global minimum $c^*(j_0)$ of (2.7) for each fixed j_0, i.e., we take $c = c^*(j_0) = \arg\min_c J(\phi(j_0, c))$ [3]. Hence we can formulate an equivalent optimization problem as follows: minimize the shape functional (2.7), where $\phi \in W^1_0(\Omega)$ depends implicitly on j_0 only, by solving the following problem:

$$\left\{\begin{array}{rll} -\Delta\phi & = \mu_0 j_0 & \text{in } \Omega\,, \\ \dfrac{\partial\phi}{\partial n} & = \varkappa\,\bar{p} - d(j_0) & \text{on } \Gamma\,, \\ \displaystyle\int_\Gamma \phi\, ds & = 0\,. & \end{array}\right. \tag{2.10}$$

Problem (2.10) is well-posed, as rigorously stated in the following lemma.

Lemma 1. *Given $b \in L_2(\Omega)$, $q \in L_2(\Gamma)$ and $c \in \mathbb{R}$, satisfying the compatibility condition $\int_\Omega b\, dx + \int_\Gamma q\, ds = 0$, there is a unique solution $\phi \in W^1_0(\Omega)$ to the problem*

$$\left\{\begin{array}{rll} -\Delta\phi & = b & \textit{in } \Omega\,, \\ \dfrac{\partial\phi}{\partial n} & = q & \textit{on } \Gamma\,, \\ \displaystyle\int_\Gamma \phi\, ds & = c\,, & \end{array}\right. \tag{2.11}$$

which depends continuously on the problem data, i.e., there is $C \in \mathbb{R}$ such that $\|\phi\|_{W^1_0(\Omega)} \le C(\|b\|_{L_2(\Omega)} + \|q\|_{L_2(\Gamma)} + |c|)$.

Proof. Let ξ be the solution in $W^1_0(\Omega)$ of:

$$\left\{\begin{array}{rll} -\Delta\xi & = b & \text{in } \Omega\,, \\ \dfrac{\partial\xi}{\partial n} & = q & \text{on } \Gamma\,, \\ \xi(x) & = o(1) & \text{as } \|x\| \to \infty\,. \end{array}\right. \tag{2.12}$$

In the space $\{u \in W^1_0(\Omega) : u = o(1) \text{ as } \|x\| \to \infty\}$, the map $u \mapsto \|\nabla u\|_{L_2(\Omega)}$ is a norm equivalent to $\|\cdot\|_{W^1_0(\Omega)}$ [20, 28]. Therefore, the standard analysis of the variational formulation of problem (2.12) shows that there is a unique solution ξ satisfying $\|\xi\|_{W^1_0(\Omega)} \le C_1(\|b\|_{L_2(\Omega)} + \|q\|_{L_2(\Gamma)})$ for some real C_1, see [27, 21, 20, 28]. The proof of the lemma is promptly obtained using this result, considering that $\phi = \xi + |\Gamma|^{-1}(c - \int_\Gamma \xi\, ds)$. □

3. Topological derivative concept

The topological derivative measures the sensitivity of a given shape functional with respect to an infinitesimal singular domain perturbation, such as the insertion of holes, inclusions, source-terms or even cracks [29, 30, 31]. It has proved extremely useful in the treatment of a wide range of problems, see [9, 32, 33, 34, 35, 36, 37, 38, 39, 40, 41, 42]. Concerning the theoretical development of the topological asymptotic analysis, see the book by Novotny & Sokolowski [43] and the papers [44, 45, 46, 47, 48]. See also the books by Ammari and Kang [49, 50] regarding the asymptotic analysis of PDE solutions and their applications to inverse problems.

Consider that a domain Ω is subject to a non-smooth perturbation confined in a small ball $B_\varepsilon(\widehat{x})$ of radius ε and center $\widehat{x} \in \Omega$. Then, if a given shape functional $\psi(\varepsilon)$, associated to the topologically perturbed domain, admits the expansion [30]

$$\psi(\varepsilon) = \psi(0) + f_1(\varepsilon) D_T^1 \psi + f_2(\varepsilon) D_T^2 \psi + o(f_2(\varepsilon))\,, \tag{3.1}$$

where $\psi(0)$ is the shape functional value for the unperturbed domain and $f_i(\varepsilon)$, $1 \leq i \leq 2$, are positive functions such that $f_i(\varepsilon) \to 0$, and $f_2(\varepsilon)/f_1(\varepsilon) \to 0$, when $\varepsilon \to 0$, we say that the functions $\widehat{x} \mapsto D_T^i \psi(\widehat{x})$, $1 \leq i \leq 2$, are the topological derivatives of ψ at $\widehat{x}$. The term $f_1(\varepsilon) D_T^1 \psi + f_2(\varepsilon) D_T^2 \psi$ can be seen as a second order correction of $\psi(0)$ to approximate $\psi(\varepsilon)$.

3.1. **The topological derivatives calculation.** Associated to the solution ϕ of (2.10), we define the function $\phi_\varepsilon \in W_0^1(\Omega)$ solution to the following problem:

$$\left\{ \begin{array}{rll} -\Delta \phi_\varepsilon &= \mu_0 j_\varepsilon & \text{in } \Omega\,, \\ \dfrac{\partial \phi_\varepsilon}{\partial n} &= \varkappa\, \bar{p} - d(j_\varepsilon) & \text{on } \Gamma\,, \\ \displaystyle\int_\Gamma \phi_\varepsilon \, ds &= 0\,. & \end{array} \right. \tag{3.2}$$

where the perturbed electric current density j_ε is identical to j_0 everywhere in Ω except in $B_\varepsilon(\widehat{x}) \subset \Omega$, a small ball of radius ε and center $\widehat{x}$. More precisely, $j_\varepsilon = j_0 + \alpha I \chi_{B_\varepsilon(\widehat{x})}$, where I is a given current density value and $\alpha = \pm 1$ is the sign of the current density in $B_\varepsilon(\widehat{x})$.

The shape functional associated to the perturbed problem reads:

$$\psi(\varepsilon) = J(\phi_\varepsilon) = \frac{1}{2} \int_\Gamma \phi_\varepsilon^2 \, ds\,. \tag{3.3}$$

Let u^* be the fundamental solution of the Laplace operator:

$$u^*(y, x) = -\frac{1}{2\pi} \ln \|y - x\|\,. \tag{3.4}$$

Theorem 2. *For $\widehat{x} \in \Omega$, there exist ε_0 such that for all $\varepsilon < \varepsilon_0$ the following equality holds*

$$\psi(\varepsilon) = \psi(0) + f_1(\varepsilon) D_T^1 \psi + f_2(\varepsilon) D_T^2 \psi\,, \tag{3.5}$$

with the functions $f_1(\varepsilon) = \pi \varepsilon^2$, $f_2(\varepsilon) = \pi^2 \varepsilon^4$ and the topological derivatives

$$D_T^1 \psi(\widehat{x}) = \alpha \mu_0 I \int_\Gamma \phi \bar{f}_{\widehat{x}} \, ds\,, \tag{3.6}$$

$$D_T^2 \psi(\widehat{x}) = \frac{1}{2} \mu_0^2 I^2 \int_\Gamma \bar{f}_{\widehat{x}}^2 \, ds\,. \tag{3.7}$$

In (3.6)-(3.7), *$\bar{f}_{\widehat{x}}$ is a continuous function on Γ, given by*

$$\bar{f}_{\widehat{x}}(x) = u^*(\widehat{x}, x) - u^*(\bar{x}, x) + g_{\widehat{x}}(x) \quad \forall x \in \Gamma\,, \tag{3.8}$$

where $\bar{x}$ is a fixed interior point of ω and $g_{\widehat{x}} \in W_0^1(\Omega)$ is solution to:

$$\left\{ \begin{array}{rll} -\Delta g_{\widehat{x}} &= 0 & \text{in } \Omega\,, \\ \dfrac{\partial g_{\widehat{x}}}{\partial n} &= -|\Gamma|^{-1} + \dfrac{\partial u^*(\bar{x}, \cdot)}{\partial n} - \dfrac{\partial u^*(\widehat{x}, \cdot)}{\partial n} & \text{on } \Gamma\,, \\ \displaystyle\int_\Gamma g_{\widehat{x}} \, ds &= \displaystyle\int_\Gamma u^*(\bar{x}, \cdot) - u^*(\widehat{x}, \cdot) \, ds\,. & \end{array} \right. \tag{3.9}$$

Moreover, the topological derivatives $D_T^1\psi$ and $D_T^2\psi$ are Lipschitz continuous functions with respect to their argument $\widehat{x}$ in any compact $\mathcal{D} \subset \Omega$.

Proof. Lets take ε_0 small enough such that every point $x \in \Gamma$ is outside the ball $B_{\varepsilon_0}(\widehat{x})$. For some $\varepsilon < \varepsilon_0$, set $f_{\widehat{x}} = (\alpha\mu_0 I\pi\varepsilon^2)^{-1}(\phi_\varepsilon - \phi) \in W_0^1(\Omega)$. Taking into account (2.10), (3.2), (3.10) and the fact that $d(j_\varepsilon) = d(j_0) + |\Gamma|^{-1}\alpha\mu_0 I\pi\varepsilon^2$, we have that $f_{\widehat{x}}$ solves:

$$\left\{\begin{array}{rll} -\Delta f_{\widehat{x}} & = (\pi\varepsilon^2)^{-1}\chi_{B_\varepsilon(\widehat{x})} & \text{in } \Omega\,, \\ \dfrac{\partial f_{\widehat{x}}}{\partial n} & = -|\Gamma|^{-1} & \text{on } \Gamma\,, \\ \displaystyle\int_\Gamma f_{\widehat{x}}\, ds & = 0\,. & \end{array}\right. \tag{3.10}$$

A particular solution to (3.10) is $f_{\widehat{x}}^p$ given by

$$f_{\widehat{x}}^p(x) = (\pi\varepsilon^2)^{-1}\int_{B_\varepsilon(\widehat{x})} u^*(y,x)\,dy - u^*(\bar{x},x)\,. \tag{3.11}$$

This last expression can be integrated exactly for each point x outside the ball $B_\varepsilon(\widehat{x})$. In particular, for each $x \in \Gamma$ we have $f_{\widehat{x}}^p(x) = u^*(\widehat{x},x) - u^*(\bar{x},x)$. Then, the solution of (3.10) is $f_{\widehat{x}} = f_{\widehat{x}}^p + g_{\widehat{x}}$ where $g_{\widehat{x}}$ is the solution to (3.9). We now take $\bar{f}_{\widehat{x}} = f_{\widehat{x}}|_\Gamma$ and (3.8) holds. Since $g_{\widehat{x}}$ does not depend on ε, (3.8) shows that $\bar{f}_{\widehat{x}}$ does not depend on ε too. Since Γ is of class C^2, and the boundary data in (3.9) is continuous, $g_{\widehat{x}} \in C^1(\overline{\Omega})$ [21]. Hence, $g_{\widehat{x}}|_\Gamma$ and then $\bar{f}_{\widehat{x}}$ are continuous. The complete topological asymptotic expansion of the shape functional becomes

$$\begin{aligned}\psi(\varepsilon) = J(\phi_\varepsilon) &= \frac{1}{2}\int_\Gamma (\phi + \alpha\mu_0 I\pi\varepsilon^2 f_{\widehat{x}})^2\,ds \\ &= \psi(0) + \pi\varepsilon^2\left(\alpha\mu_0 I\int_\Gamma \phi\bar{f}_{\widehat{x}}\,ds\right) + \pi^2\varepsilon^4\left(\frac{1}{2}\mu_0^2 I^2\int_\Gamma \bar{f}_{\widehat{x}}^2\,ds\right),\end{aligned} \tag{3.12}$$

where the expressions inside the parentheses depend on $\widehat{x}$ but do not depend on ε, hence being the first and second order topological derivatives of ψ. To show that these derivatives are Lipschitz in $\mathcal{D}$, the Cauchy–Schwartz inequality applied to (3.6)-(3.7) gives

$$|D_T^1\psi(\widehat{x}) - D_T^1\psi(\widehat{y})| \le \mu_0 I\|\phi\|_{L_2(\Gamma)}\|f_{\widehat{x}} - f_{\widehat{y}}\|_{L_2(\Gamma)}\,, \tag{3.13}$$

$$|D_T^2\psi(\widehat{x}) - D_T^2\psi(\widehat{y})| \le \frac{1}{2}\mu_0^2 I^2\|f_{\widehat{x}} + f_{\widehat{y}}\|_{L_2(\Gamma)}\|f_{\widehat{x}} - f_{\widehat{y}}\|_{L_2(\Gamma)}\,. \tag{3.14}$$

Note that the existence of the norms in (3.13)–(3.14) is ensured by the trace theorem applied to the functions ϕ, $f_{\widehat{x}}$ and $f_{\widehat{y}}$ of $W_0^1(\Omega)$. Then, since $\|f_{\widehat{x}} + f_{\widehat{y}}\|_{L_2(\Gamma)} \le \|f_{\widehat{x}}\|_{L_2(\Gamma)} + \|f_{\widehat{y}}\|_{L_2(\Gamma)}$, the continuity property follows from

(i) $\|f_{\widehat{x}}\|_{L_2(\Gamma)}$ is bounded in $\mathcal{D}$,

(ii) $\|f_{\widehat{x}} - f_{\widehat{y}}\|_{L_2(\Gamma)} \le C\|\widehat{x} - \widehat{y}\|$ for some $C \in \mathbb{R}$, with $\widehat{x}, \widehat{y} \in \mathcal{D}$.

Note that (ii) implies the continuity of the map $\widehat{x} \mapsto f_{\widehat{x}}|_\Gamma$, for the norm $\|\cdot\|_{L_2(\Gamma)}$, so that (ii) implies (i). To prove (ii) we use (3.8) to obtain

$$\|\bar{f}_{\widehat{x}} - \bar{f}_{\widehat{y}}\|_{L_2(\Gamma)} \le \|u(\widehat{x},\cdot) - u(\widehat{y},\cdot)\|_{L_2(\Gamma)} + \|g_{\widehat{x}} - g_{\widehat{y}}\|_{L_2(\Gamma)}\,, \tag{3.15}$$

where $g_{\widehat{x}} - g_{\widehat{y}} \in W_0^1(\Omega)$ is solution to

$$\left\{\begin{array}{rll} -\Delta(g_{\widehat{x}} - g_{\widehat{y}}) & = 0\,, & \text{in } \Omega\,, \\ \dfrac{\partial(g_{\widehat{x}} - g_{\widehat{y}})}{\partial n} & = -\left(\dfrac{\partial u^*(\widehat{x},\cdot)}{\partial n} - \dfrac{\partial u^*(\widehat{y},\cdot)}{\partial n}\right) & \text{on } \Gamma\,, \\ \displaystyle\int_\Gamma (g_{\widehat{x}} - g_{\widehat{y}})\,ds & = -\displaystyle\int_\Gamma u^*(\widehat{x},\cdot) - u^*(\widehat{y},\cdot)\,ds\,. & \end{array}\right. \tag{3.16}$$

By the trace theorem we have $\|g_{\widehat{x}} - g_{\widehat{y}}\|_{L_2(\Gamma)} \leq C_1 \|g_{\widehat{x}} - g_{\widehat{y}}\|_{W_0^1(\Omega)}$ for some $C_1 \in \mathbb{R}$. Hence (3.15) and Lemma 1 applied to (3.16) give

$$\|\bar{f}_{\widehat{x}} - \bar{f}_{\widehat{y}}\|_{L_2(\Gamma)} \leq C_2 \|u(\widehat{x},\cdot) - u(\widehat{y},\cdot)\|_{L_2(\Gamma)} + C_3 \left\| \frac{\partial u^*(\widehat{x},.)}{\partial n} - \frac{\partial u^*(\widehat{y},.)}{\partial n} \right\|_{L_2(\Gamma)}, \tag{3.17}$$

for some $C_2, C_3 \in \mathbb{R}$. Result (ii) is obtained from the previous inequality and the fact that $\Gamma \in C^2$, so that u^* and $\partial u^*/\partial n$ are continuous and differentiable with respect to both variables in the compact $\mathcal{D} \times \Gamma$, hence they are Lipschitz in $\mathcal{D} \times \Gamma$. □

Instead of using (3.6), the first order topological derivative can be computed efficiently by using the adjoint state v, see [3],

$$D_T^1 \psi(\widehat{x}) = -\alpha \mu_0 I v(\widehat{x}), \tag{3.18}$$

where v is the unique solution in $W_0^1(\Omega)$ to the following problem:

$$\begin{cases} -\Delta v &= 0, \\ \dfrac{\partial v}{\partial n} &= -\phi \quad \text{on } \Gamma, \\ \displaystyle\int_\Gamma v\, ds &= 0. \end{cases} \tag{3.19}$$

Remark 3. *Note that* (3.18) *allows us to compute the first order topological derivative at several points by solving once the boundary value problem* (3.19)*. For the second order derivatives, the boundary value problem* (3.9) *must be solved once for each point* $\widehat{x}$*. However, note that unlike the solution to* (3.19)*, the solution to* (3.9) *does not depend on* ϕ*, and then it does not depend on the actual current density distribution* j_0*. Therefore, second order derivatives can be computed once before starting the optimization process. In addition, the point* $\widehat{x}$ *only affects the right hand side of the linear systems of the numerical approach, thus evaluation of second order derivatives requires of only one factorization. Hence, the computational cost of evaluation of second order derivatives is much lower than the usual case where they must be computed at each iteration, requiring the factorization of different coefficient matrices.*

We end this section with the following result:

Theorem 4. *Given a centrally symmetric domain* ω*, i.e. simmetric with respect to the center* $\bar{x}$ *interior to* ω*, then the topological derivative* $D_T^2\psi(x) > 0$ *for all* $x \in \Omega$*.*

Proof. According to (3.7), $D_T^2\psi(x) \geq 0$, for all $x \in \Omega$ and hence we just have to prove that there is no point $\widehat{x}$ such that $D_T^2\psi(\widehat{x}) = 0$. Let us assume that a point $\widehat{x} \in \Omega$ satisfying $D_T^2\psi(\widehat{x}) = 0$ exists. Hence, according to (3.7), the solution f of (3.10) satisfies $f(x) = 0$ for all $x \in \Gamma$. We know that there exists a constant c such that the solution $g_{\widehat{x}}$ to (3.9) satisfies the growth condition $g_{\widehat{x}}(x) = c + o(1)$ [21]. Therefore, since outside $B_\varepsilon(\widehat{x})$ we have $f_0(x) = u^*(\widehat{x}, x) - u^*(\bar{x}, x)$, f satisfies the same growth condition for the same c. Therefore, f should be a solution in $W_0^1(\Omega)$ to the following problem:

$$\begin{cases} -\Delta f &= (\pi\varepsilon^2)^{-1} \chi_{B_\varepsilon(\widehat{x})} & \text{in } \Omega, \\ f &= 0 & \text{on } \Gamma, \\ \dfrac{\partial f}{\partial n} &= -|\Gamma|^{-1} & \text{on } \Gamma, \\ f(x) &= c + o(1) & \text{as } \|x\| \to \infty. \end{cases} \tag{3.20}$$

On the other hand, due to the growth condition satisfied by f, the following boundary integral equation holds for each function $q : \Omega \to \mathbb{R}$ satisfying $\Delta q(x) = 0$ in Ω and $q(x) = o(1)$ as $\|x\| \to \infty$:

$$\int_{B_\varepsilon(\widehat{x})} (\pi\varepsilon^2)^{-1} q(x)\, dx = \int_\Gamma f \frac{\partial q}{\partial n}\, ds - \int_\Gamma \frac{\partial f}{\partial n} q\, ds. \tag{3.21}$$

By using the mean value property of harmonic functions, and by replacing the boundary values of f into (3.21) we have

$$q(\widehat{x}) = |\Gamma|^{-1} \int_\Gamma q \, ds \,. \tag{3.22}$$

Consider a Cartesian coordinate system with $\bar{x}$ as its origin. Let (x_1, x_2) be the coordinates of $x \in \Omega$ and let the functions q_1 and q_2 be defined as

$$q_1(x) = \frac{x_1}{r^2} \,, \quad q_2(x) = \frac{x_2}{r^2} \,, \tag{3.23}$$

with $r^2 = x_1^2 + x_2^2$. Since q_1 and q_2 satisfy the hypothesis required for q, (44) gives for these functions

$$\frac{\widehat{x}_1}{\widehat{r}^2} = |\Gamma|^{-1} \int_\Gamma \frac{x_1}{r^2} \, ds \,, \quad \frac{\widehat{x}_2}{\widehat{r}^2} = |\Gamma|^{-1} \int_\Gamma \frac{x_1}{r^2} \, ds \,, \tag{3.24}$$

where $(\widehat{x}_1, \widehat{x}_2)$ are the coordinates of $\widehat{x}$ and $\widehat{r}^2 = \widehat{x}_1^2 + \widehat{x}_2^2$. By hypothesis $\widehat{x} \in \Omega$, hence $\widehat{r}^2 > 0$ and at least one of $q_1(\widehat{x})$ and $q_2(\widehat{x})$ is non-zero. However, both integral expressions of (3.24) vanish because of the central symmetry of Γ. Since there is a contradiction, a point $\widehat{x} \in \Omega$ satisfying $D_T^2 \psi(\widehat{x}) = 0$ does not exist. □

4. A topological derivative-based level-set algorithm

In this section we state a level-set topology design algorithm based on the topological derivatives obtained in the previous section. First we consider domains Ω which possess central symmetry. In this case we can devise a level set algorithm to generate a sequence of current density functions j_0 satisfying (2.2) at each iteration. In the general case, condition (2.2) can not be ensured automatically, and a penalty function strategy to enforce the satisfaction of this constraint will be followed.

4.1. **The symmetric case.**

In this case the current density j_0 is sought as the solution of the general optimization problem stated as

$$\underset{\substack{j_0 \in \mathcal{O} \\ \int_\Omega j_0 \, dx = 0}}{\text{Minimize}} \, J(\phi) \,, \tag{4.1}$$

where $\mathcal{O}$ is the set of functions $j_0 = I(\chi_{\Theta^+} - \chi_{\Theta^-})$ with χ_{Θ^+} and χ_{Θ^-} being the characteristic functions of the sets Θ^+ and Θ^-, which are the open and disjoints parts of Ω representing the regions where the current density j_0 is, respectively, positive or negative. We assume that Θ^+ and Θ^- are in a compact $\Theta \subset \Omega$. The function ϕ is the solution of (2.8) in $W_0^1(\Omega)$. Therefore, the design variables of problem (4.1) are the shape and topology of Θ^+ and Θ^-.

According to the topological expansion (3.12), the introduction of a circular region of current density αI, $\alpha \in \{+1, -1\}$, and center $\widehat{x} \in \Omega$ changes the value of the objective function of problem (4.1). If we consider an optimal configuration of inductors with respect to the class of perturbations we are analyzing, the introduction of that small circular region at $\widehat{x} \in \Omega^0 = \Omega \setminus (\overline{\Theta^+} \cup \overline{\Theta^-})$ should not increase the objective function. Hence, according to the expression (3.18) of the first order topological derivative, the optimal configuration should satisfy the following necessary condition:

$$-\alpha \mu_0 I v(\widehat{x}) \geq 0 \quad \forall \widehat{x} \in \Omega^0 \,. \tag{4.2}$$

Since α could be positive or negative, for the optimal configuration we have

$$v(\widehat{x}) = 0 \quad \forall \widehat{x} \in \Omega^0 \,. \tag{4.3}$$

However, since v is harmonic, by the identity theorem of harmonic functions [51], v vanishes on the entire domain Ω, and by (3.18) we have, for the optimal configuration:

$$D_T^1 \psi = 0 \quad \text{in } \Omega \,. \tag{4.4}$$

Now we are ready to devise e topological derivative-based optimization algorithm to solve problem (4.1) based on the ideas in [9], that have been successfully applied to several problems.

The procedure relies on a level-set domain representation of Θ^+ and Θ^- [52], and the approximation of the topological optimality conditions through a fixed point iteration. The main difficulty of applying the ideas in [9] to the present case is that the first order topological derivative vanishes at the solution according to (4.4). The novelty of our algorithm is that it considers the expected variation of the objective functional given by the topological expansion (3.12) instead of the first order topological derivative to define the level sets.

With the adoption of a level-set domain representation, the region Θ^+ is characterized by a function $\psi^+ \in L^2(\Theta)$ such that

$$\Theta^+ = \{x \in \Theta,\ \psi^+(x) < 0\}\,, \tag{4.5}$$

whereas the region Θ^- is characterized by a function $\psi^- \in L^2(\Theta)$:

$$\Theta^- = \{x \in \Theta,\ \psi^-(x) < 0\}\,. \tag{4.6}$$

Let $EV(\widehat{x}, \varepsilon, \alpha)$ be the expected variation of the objective function of problem (4.1) for a perturbation of j_0 consisting in a circular region of current density αI of radius ε and center $\widehat{x}$, namely,

$$EV(\widehat{x}, \varepsilon, \alpha) = f_1(\varepsilon) D_T^1 \psi(\widehat{x}) + f_2(\varepsilon) D_T^2 \psi(\widehat{x})\,. \tag{4.7}$$

Take $\Theta^0 = \Theta \backslash (\overline{\Theta^+} \bigcup \overline{\Theta^-})$. A sufficient condition of local optimality for the class of perturbations considered is that the expected variation of the objective function be positive, i.e.,

$$EV(\widehat{x}, \varepsilon, \alpha) > 0\,, \quad \forall \widehat{x} \in \Theta^+\,, \text{ and } \alpha = -1\,, \tag{4.8}$$

$$EV(\widehat{x}, \varepsilon, \alpha) > 0\,, \quad \forall \widehat{x} \in \Theta^-\,, \text{ and } \alpha = +1\,, \tag{4.9}$$

$$EV(\widehat{x}, \varepsilon, \alpha) > 0\,, \quad \forall \widehat{x} \in \Theta^0\,, \text{ and } \alpha = \pm 1\,. \tag{4.10}$$

Following [9], to devise a level-set-based algorithm whose aim is to produce a topology that satisfies (4.8)–(4.10), we choose a value for ε (in the numerical approach we define a mesh of cells in the domain Θ and take a value ε related to the size of the cells) and define the functions

$$g^+(x) = \begin{cases} -EV(\widehat{x}, \varepsilon, -1) & \text{if } \widehat{x} \in \Theta^+\,, \\ EV(\widehat{x}, \varepsilon, +1) & \text{if } \widehat{x} \in \Theta^0 \cup \Theta^-\,, \end{cases} \tag{4.11}$$

$$g^-(x) = \begin{cases} -EV(\widehat{x}, \varepsilon, +1) & \text{if } \widehat{x} \in \Theta^-\,, \\ EV(\widehat{x}, \varepsilon, -1) & \text{if } \widehat{x} \in \Theta^0 \cup \Theta^+\,. \end{cases} \tag{4.12}$$

With the above definitions and (4.5)–(4.6), it can be easily established that the sufficient conditions (4.8)–(4.10) are satisfied if the following equivalence relations between the functions g^+ and g^- and the level-set functions ψ^+ and ψ^- hold

$$\exists\, \tau^+ > 0 \quad \text{s.t.} \quad h(g^+) = \tau^+ \psi^+\,, \tag{4.13}$$

$$\exists\, \tau^- > 0 \quad \text{s.t.} \quad h(g^-) = \tau^- \psi^-\,, \tag{4.14}$$

where $h : \mathbb{R} \to \mathbb{R}$ must be an odd and strictly increasing function, e.g.,

$$h(x) = \text{sign}(x)|x|^\beta \quad \text{with } \beta > 0\,. \tag{4.15}$$

In fact, if $\widehat{x} \in \Theta^+$, then $\psi^+(\widehat{x}) < 0$. By (4.13) and since h preserves the sign we have $g^+(\widehat{x}) < 0$, and by (4.11) we have $EV(\widehat{x}, \varepsilon, -1) > 0$, proving (4.8). The proofs of (4.9) and (4.10) are analogous considering $\widehat{x}$ respectively in Θ^- and Θ^0.

Conditions (4.13)–(4.14) can be expressed equivalently as

$$\theta^+ := \arccos\left[\frac{\langle h(g^+), \psi^+ \rangle_{L^2(\Theta)}}{\|h(g^+)\|_{L^2(\Theta)}\, \|\psi^+\|_{L^2(\Theta)}}\right] = 0\,, \tag{4.16}$$

$$\theta^- := \arccos\left[\frac{\langle h(g^-), \psi^- \rangle_{L^2(\Theta)}}{\|h(g^-)\|_{L^2(\Theta)}\, \|\psi^-\|_{L^2(\Theta)}}\right] = 0\,, \tag{4.17}$$

where θ^+ is the angle between the vectors $h(g^+)$ and ψ^+ in $L^2(\Theta)$ and θ^- is the counterpart between $h(g^-)$ and ψ^-.

To find the optimal Θ^+ (the case of Θ^- is completely analogous), we start from an initial level-set function $\psi_0^+ \in L^2(\Theta)$ which defines the initial guess. Then, the algorithm produces a sequence $(\psi_i^+)_{i\in\mathbb{N}}$ of level-set functions that provides successive approximations to the sufficient conditions of optimality. The sequence satisfies

$$\begin{array}{l} \psi_0^+ \in L^2(\Theta)\,, \\ \psi_{n+1}^+ \in \mathrm{co}(\psi_n^+, h(g_n^+)) \qquad \forall n \in \mathbb{N}\,, \end{array} \tag{4.18}$$

where $\mathrm{co}(\psi_n^+, h(g_n^+))$ is the convex hull of $\{\psi_n^+, h(g_n^+)\}$. In the actual algorithm the initial guess ψ_0^+ and subsequent iteration points can be normalized, see [9] for further details. The non-normalized sequences for both Θ^+ and Θ^- are

$$\left.\begin{array}{l} \psi_{n+1}^+ = (1-t_n)\psi_n^+ + t_n h(g_n^+) \\ \psi_{n+1}^- = (1-t_n)\psi_n^- + t_n h(g_n^-) \end{array}\right\} \quad \forall n \in \mathbb{N}\,, \tag{4.19}$$

where $t_n \in [0,1]$ is a step size determined by a line-search in order to decrease the value of the cost functional $J(\phi)$. The iterative process is stopped when certain criterion is satisfied, see Section 5. The angles θ^+ and θ^- can be use as indicators of the accuracy of (4.13) and (4.14) at the final iteration and can be used to determine the necessity of a mesh refinement [9].

The next theorem shows that the algorithm given by the update rule (4.19) is well defined, i.e., for every $t_n \in [0,1]$ the functions ψ_{n+1}^+ and ψ_{n+1}^- generate disjoint sets Θ^+ and Θ^-. We prove by induction that $\psi_n^+ + \psi_n^- \geq 0\ \forall n \in \mathbb{N}$. This latter inequality is sufficient to show that Θ^+ and Θ^- are disjoint, since a point x in both sets would satisfy $\psi_n^+(x) < 0$ and $\psi_n^-(x) < 0$ and then would satisfy $\psi_n^+(x) + \psi_n^-(x) < 0$.

Theorem 5. *Assume that $\psi_0^+ + \psi_0^- \geq 0$. Then $\psi_n^+ + \psi_n^- \geq 0\ \forall n \in \mathbb{N}$.*

Proof. According to (4.11)–(4.12) and taking into account that h is odd we have

$$h(g_n^+(x)) + h(g_n^-(x)) = 0 \quad \forall x \in \Theta^+ \cup \Theta^-\,. \tag{4.20}$$

In addition, for a point $x \in \Theta^0$ we have

$$g_n^+(x) + g_n^-(x) = EV(x,\varepsilon,+1) + EV(x,\varepsilon,-1)\,, \tag{4.21}$$

and, according to (4.7) and (3.18),

$$g_n^+(x) + g_n^-(x) = 2f_2(\varepsilon) D_T^2 \psi(x) \geq 0\,, \tag{4.22}$$

hence $g_n^+(x) \geq -g_n^-(x)$ and, since h is strictly increasing,

$$h(g_n^+(x)) \geq h(-g_n^-(x)) \quad \forall x \in \Theta^0\,. \tag{4.23}$$

Since h is odd, the last inequality proves the desired result in Θ^0 and thanks to (4.20) also in the whole domain Θ:

$$h(g_n^+(x)) + h(g_n^-(x)) \geq 0 \quad \forall x \in \Theta\,. \tag{4.24}$$

The induction hypothesis is $\psi_n^+ + \psi_n^- \geq 0$, and by (4.19) we have

$$\psi_{n+1}^+ + \psi_{n+1}^- = (1-t_n)[\psi_n^+ + \psi_n^-] + t_n[h(g_n^+) + h(g_n^-)]\,. \tag{4.25}$$

Using the induction hypothesis and (4.24) we obtain $\psi_{n+1}^+ + \psi_{n+1}^- \geq 0$ for every $t_n \in [0,1]$. □

Remark 6. *If there is no previous information about the optimum, a suitable initial guess that satisfies the inequality $\psi_0^+ + \psi_0^- \geq 0$ is $\psi_0^+ = \psi_0^- = 1$, which corresponds to zero positive and negative currents.*

4.2. **The asymmetric case.** In the asymmetric case the satisfaction of condition (2.2) cannot be ensured automatically by the algorithm described in the previous section. In fact, in Section 5 we present an example where the algorithm fails to find a solution satisfying (2.2).

In the asymmetric case we propose to relax this constraint and minimize the following penalty function:

$$P(0) = J(\phi) + \frac{1}{2}\rho\, d(j_0)^2\,, \tag{4.26}$$

where $\rho > 0$ is a penalty parameter. Hence, in the penalty approach the current density j_0 is sought as the solution of the following optimization problem:

$$\underset{j_0 \in \mathcal{O}}{\text{Minimize}}\, J(\phi) + \frac{1}{2}\rho d(j_0)^2\,. \tag{4.27}$$

In this case, since $d(j_\varepsilon) = d(j_0) + |\Gamma|^{-1}\alpha\mu_0 I\pi\varepsilon^2$, it is not difficult to see that P admits the topological expansion (3.1), with the same functions f_1 and f_2 as ψ, and with the following topological derivatives:

$$D_T^1 P(\widehat{x}) = D_T^1\psi(\widehat{x}) + \rho\alpha\mu_0 I|\Gamma|^{-1} d(j_0)\,, \tag{4.28}$$

$$D_T^2 P(\widehat{x}) = D_T^2\psi(\widehat{x}) + \frac{1}{2}\rho\mu_0^2 I^2|\Gamma|^{-2}\,. \tag{4.29}$$

Note that, as well as the symmetric case, the second order topological derivative $D_T^2 P(\widehat{x})$ is strictly positive thanks to the strictly positive penalty term.

The topology optimization procedure proposed to solve asymmetric problems is the same as in the previous section, using the penalty function (4.26) as objective and the expected variation $EV(x, \varepsilon, \alpha)$ computed according to the topological derivatives (4.28)–(4.29).

5. Numerical examples

Four examples are presented. The first two have known solutions, since the target shapes considered are equilibrium shapes for given current density distributions. The second example considers an asymmetric target shape, so that it serves to evaluate the effect of the penalty term proposed in Section 4.2. The last two examples consist of more realistic design problems. The boundary element method used in [3] was applied here to solve the boundary value problems and to compute approximately the first and second order topological derivatives. For all the examples we consider $\sigma = 1.0 \times 10^{-4}$ and $\mu_0 = 1.0$. Two meshes are considered; the case (a) has cells of size 0.02 and the case (b) has cells of size 0.02, see Table 1. The optimization procedure stops when in subsequent iterations we have the same configuration of inductors, i.e., the level sets contains the same cells.

Table 1. Examples

Example	NE	NC	SC	I
Ex1a	120	4724	0.05	0.4
Ex1b	120	29520	0.02	0.4
Ex2a	169	4715	0.05	0.4
Ex2b	169	29463	0.02	0.4
Ex3a	152	10228	0.05	0.2
Ex3b	152	64120	0.02	0.2
Ex4a	172	11708	0.05	0.15
Ex4b	172	73420	0.02	0.15

NE: number of boundary elements, NC: number of domain cells, SC: size of the cells.

The target shape of the first example is the solution of a direct free-surface problem for a liquid metal column of cross-section area $S_0 = \pi$, considering six distributed currents of density $I = 0.4$ as shown in Fig. 1, see Fig. 1. The result obtained for finer mesh is shown in Fig. 2. The evolution of the objective function along the iterative process is shown in Fig. 3.

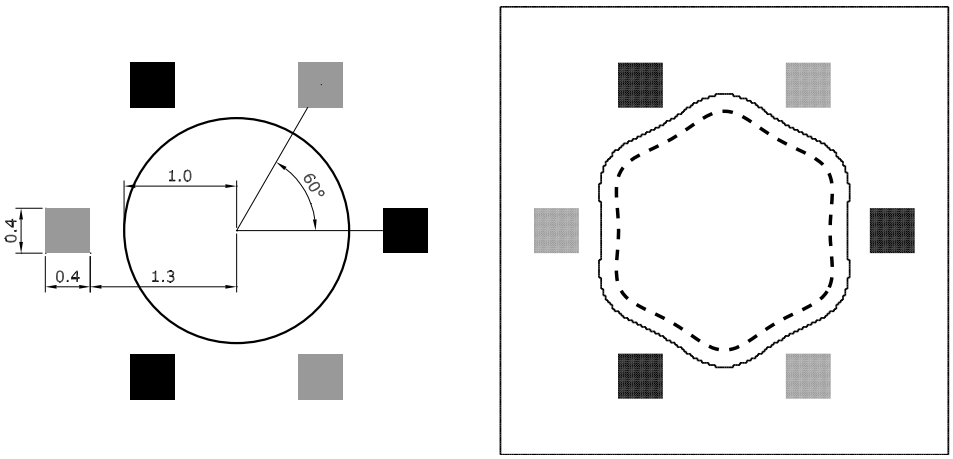

FIGURE 1. Example 1. (a) Initial configuration of the direct free-surface problem. (b) Target shape and exact solution. Black area: positive inductors, gray area: negative inductors, dashed line: target shape, thin solid line: boundary of the mesh of cells.

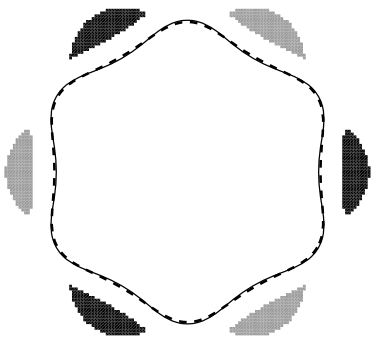

FIGURE 2. Example 1. Solution for a mesh of cells of size 0.02 with $\beta = 3$. Black area: positive inductors, gray area: negative inductors, dashed line: target shape, thin solid line: equilibrium shape.

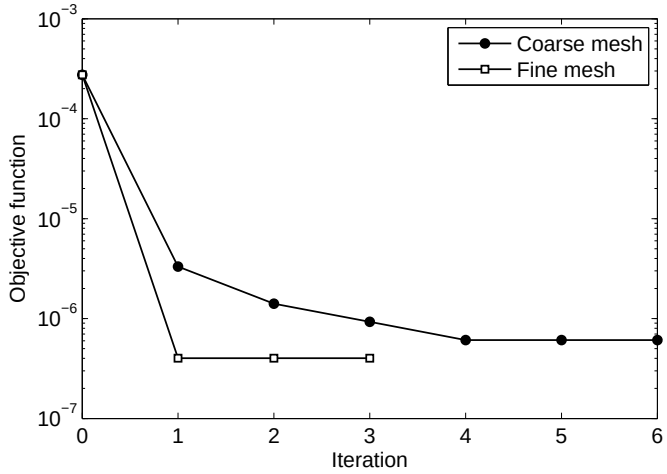

FIGURE 3. Example 1. Evolution of the objective function for $\beta = 3$.

In the second example we move the inductors to generate an asymmetric objective shape as shown in Fig. 4. The result obtained for the finer mesh is shown in Fig. 5. The evolution of the objective function along the iterative process is shown in Fig. 6 and the evolution of the total current considering three different values of the penalty parameter ρ is shown in Fig. 7. Note that from the eighth iteration the effect of the penalty term is noticeable. For $\rho = 0$ the total current never stop increasing, and for $\rho = 1.0 \times 10^{-11}$ the total current converges to zero. The value $\rho = 1.0 \times 10^{-12}$ is not large enough to produce a significant reduction of the total current.

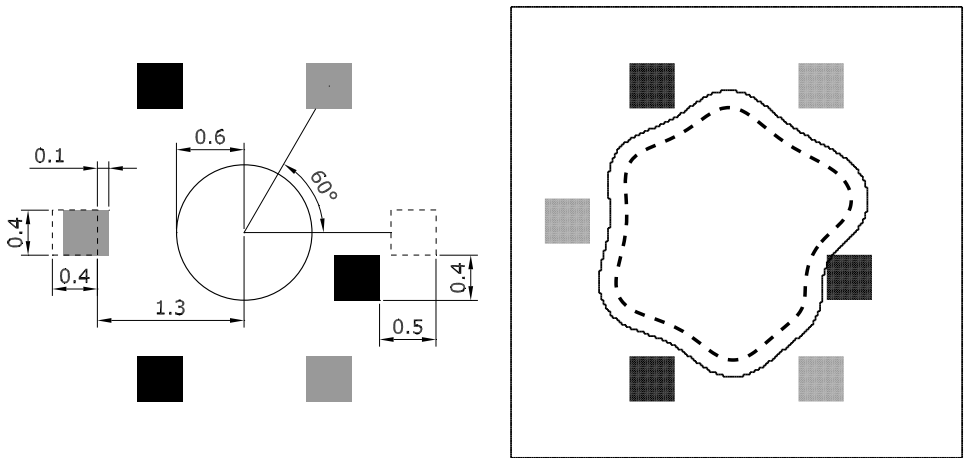

(a) (b)

FIGURE 4. Example 2. (a) Initial configuration of the direct free-surface problem. (b) Target shape and exact solution. Black area: positive inductors, gray area: negative inductors, dashed line: target shape, thin solid line: boundary of the mesh of cells.

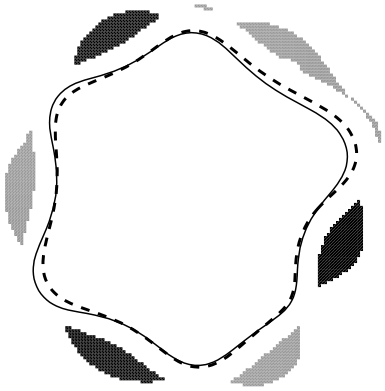

FIGURE 5. Example 2. Solution for a mesh of cells of size 0.02 with $\beta = 3$ and $\rho = 1.0 \times 10^{-11}$. Black area: positive inductors, gray area: negative inductors, dashed line: target shape, thin solid line: equilibrium shape.

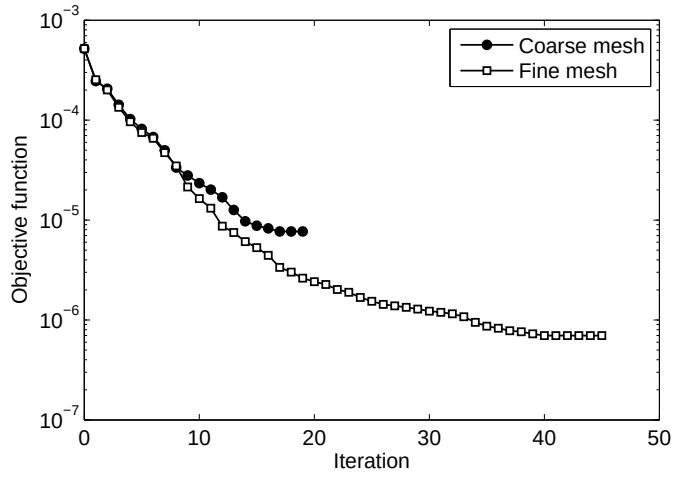

FIGURE 6. Example 2. Evolution of the objective function for $\beta = 3$ and $\rho = 1 \times 10^{-11}$.

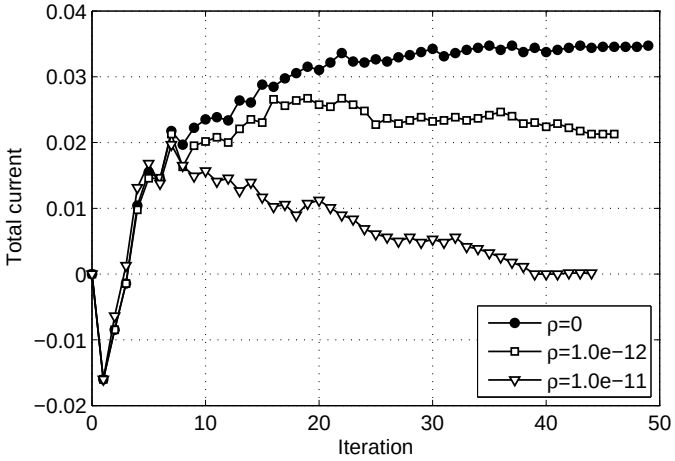

FIGURE 7. Example 2. Evolution of the total current considering different values of ρ.

The third example is depicted in Fig. 8. The result obtained for the finer mesh is shown in Fig. 9. The evolution of the objective function along the iterative process is shown in Fig. 10.

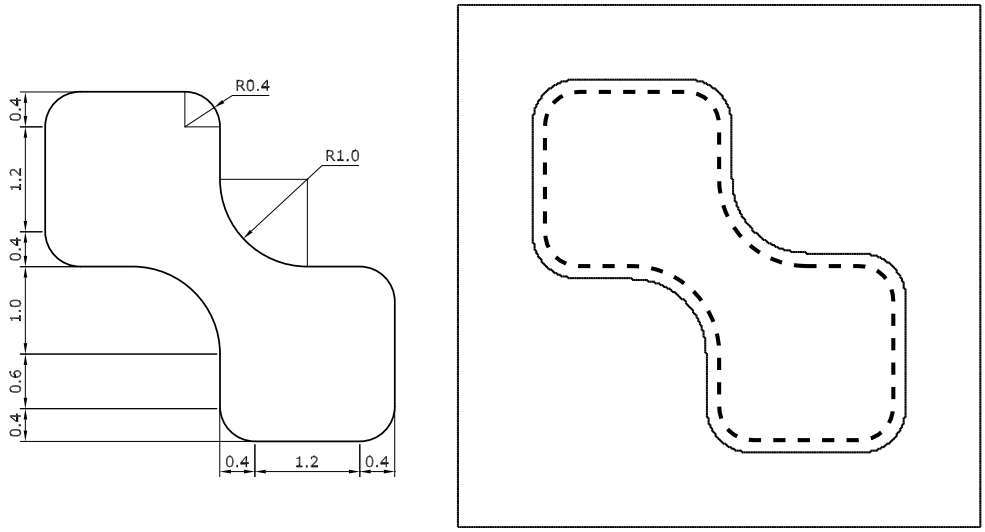

(a) (b)

FIGURE 8. Example 3. (a) Description of the problem geometry. (b) Target shape. Dashed line: target shape, thin solid line: boundary of the mesh of cells.

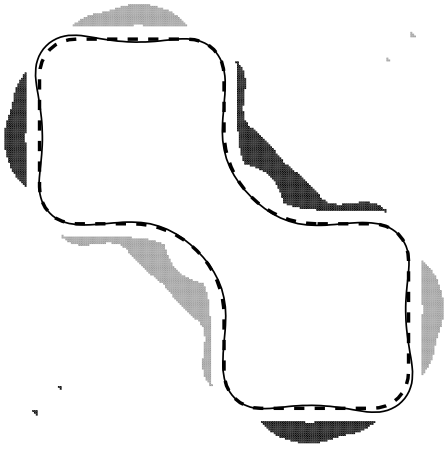

FIGURE 9. Example 3. Solution for a mesh of cells of size 0.02 and $\beta = 3$. Black area: positive inductors, gray area: negative inductors, dashed line: target shape, thin solid line: equilibrium shape.

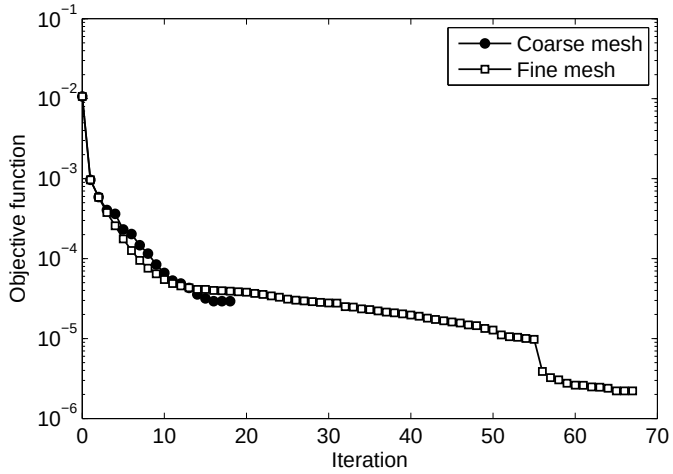

FIGURE 10. Example 3. Evolution of the objective function for $\beta = 3$.

In the last example we consider the asymmetric target shape of Fig. 11. For this example, the compatibility equation (2.6) is satisfied if the sign of $\varkappa$ does not change at the two vertices indicated in Fig. 11. The result obtained for the finer mesh is shown in Fig. 12. The evolution of the objective function along the iterative process is shown in Fig. 13 and the evolution of the total current considering three different values of the penalty parameter ρ is shown in Figs 14. Note that the total current of the solution depends on ρ as in Example 2. Solutions with almost zero total current are found for $\rho = 1.0 \times 10^{-11}$.

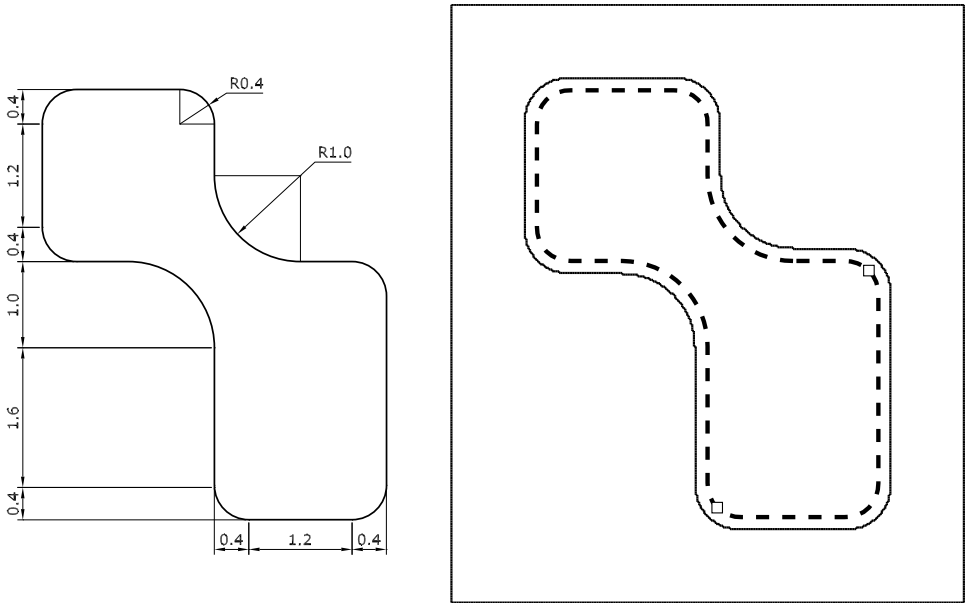

(a) (b)

FIGURE 11. Example 4. (a) Description of the problem geometry. (b) Target shape. Dashed line: target shape, thin solid line: boundary of the mesh of cells, white squares: points where the sign remains unchanged.

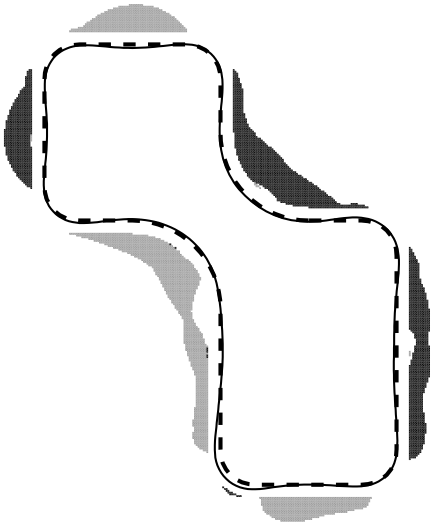

FIGURE 12. Example 4. Solution for a mesh of cells of size 0.02 and $\beta = 3$. Black area: positive inductors, gray area: negative inductors, dashed line: target shape, thin solid line: equilibrium shape.

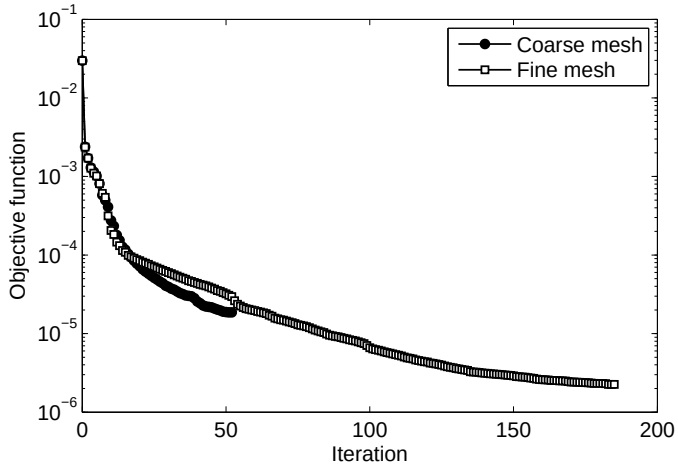

FIGURE 13. Example 4. Evolution of the objective function for $\beta = 3$.

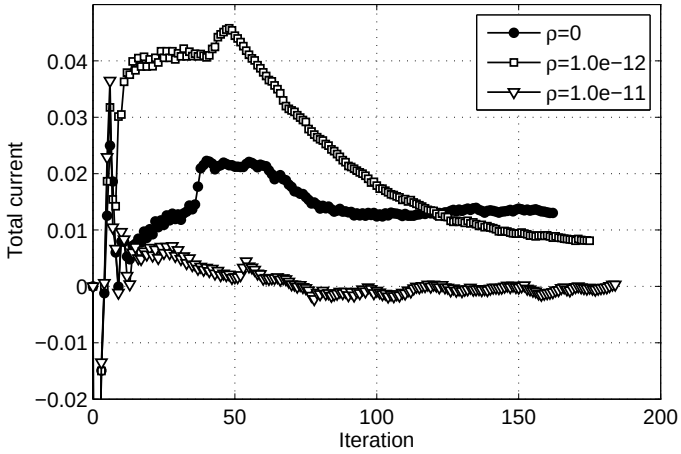

FIGURE 14. Example 4. Evolution of the total current considering different values of ρ.

5.1. **Results summary.** Table 2 resumes the information about the examples considered. For each example the number of iterations performed by the optimization algorithm proposed in [3] is indicated, as well as those performed by the present algorithm for the values $\beta = 1$ and $\beta = 3$ in (4.15). In the case of the asymmetric examples, the results obtained for $\rho = 1.0 \times 10^{-11}$ are given. Table 2 shows that, for these examples, the present optimization algorithm with $\beta = 3$ was generally the most efficient. Note that the solutions of Examples 2 and 4 required a relatively large number of iterations when compared to the similar symmetric Examples 1 and 3. However, for both asymmetric examples the penalty approach was effective to find suitable solutions.

TABLE 2. Results summary

Example	IterP	Iter1	Iter3	IOF	FOF3
Ex1a	24	4	6	2.747e-04	6.088e-07
Ex1b	47	4	3	2.747e-04	4.009e-07
Ex2a	21	17	19	5.187e-04	7.698e-06
Ex2b	63	61	45	5.187e-04	6.977e-07
Ex3a	29	18	18	1.066e-02	2.936e-05
Ex3b	108	134	67	1.066e-02	2.219e-06
Ex4a	53	56	52	2.976e-02	4.248e-05
Ex4b	145	190	184	2.976e-02	2.257e-06

IterP: number of iterations performed by the algorithm proposed in [3], Iter1: number of iterations performed by the level set algorithm for $\beta = 1$, Iter3: number of iterations performed by the level set algorithm for $\beta = 3$, IOF: initial value of the objective function, FOF3: final value of the objective function for $\beta = 3$.

6. CONCLUSIONS

We have proposed a new method for the topology design of inductors in electromagnetic casting. The method is based on a topology optimization formulation and uses level-sets together with first and second order topological derivatives to design suitable inductors.

The complete asymptotic expansion of the objective functional regarding the introduction of a small inductor was derived in this paper, generalizing the results of [3]. We have shown that the first order topological derivative vanishes at the solution, precluding the direct application

of the topology optimization algorithm proposed by Amstutz & Andrä [9] to the studied optimization problem. However, we have shown how to circumvent this difficulty using second order topological derivatives.

In the case of centrally symmetric geometries, the method proposed generates a sequence of solutions satisfying all the equality constraints. A penalty-based approach was proposed for problems with asymmetric geometries.

The set of examples considered show that the method proposed is effective and efficient, and therefore can be successfully used in the design of inductors in electromagnetic casting.

Acknowledgements

The authors thank the Brazilian Research Councils CAPES, CNPq and FAPERJ, the Uruguayan Councils ANII and CSIC and the French Research Councils COFECUB, INRIA and CNRS for the financial support.

References

[1] A. Canelas, J. R. Roche, J. Herskovits, The inverse electromagnetic shaping problem, Structural and Multidisciplinary Optimization 38 (4) (2009) 389–403. doi:10.1007/s00158-008-0285-9.

[2] A. Canelas, J. R. Roche, J. Herskovits, Inductor shape optimization for electromagnetic casting, Structural and Multidisciplinary Optimization 39 (6) (2009) 589–606. doi:10.1007/s00158-009-0386-0.

[3] A. Canelas, A. A. Novotny, J. R. Roche, A new method for inverse electromagnetic casting problems based on the topological derivative, Journal of Computational Physics 230 (9) (2011) 3570–3588. doi:10.1016/j.jcp.2011.01.049.

[4] J. R. Roche, J. Sokołowski, Numerical methods for shape identification problems, Control and Cybernetics 25 (5) (1996) 867–894, shape optimization and scientific computations (Warsaw, 1995).

[5] A. Friedman, M. Vogelius, Identification of small inhomogeneities of extreme conductivity by boundary measurements: a theorem on continuous dependence, Archive for Rational Mechanics and Analysis 105 (4) (1989) 299–326. doi:10.1007/BF00281494.

[6] R. Kohn, M. Vogelius, Determining conductivity by boundary measurements, Communications on Pure and Applied Mathematics 37 (3) (1984) 289–298. doi:10.1002/cpa.3160370302.

[7] M. Brühl, M. Hanke, M. S. Vogelius, A direct impedance tomography algorithm for locating small inhomogeneities, Numerische Mathematik 93 (4) (2003) 635–654. doi:10.1007/s002110200409.

[8] K. Eppler, H. Harbrecht, On a kohn-vogelius like formulation of free boundary problems, Computational Optimization and Applications Online. doi:10.1007/s10589-010-9345-3.

[9] S. Amstutz, H. Andrä, A new algorithm for topology optimization using a level-set method, Journal of Computational Physics 216 (2) (2006) 573–588. doi:10.1016/j.jcp.2005.12.015.

[10] C. Zhiqiang, J. Fei, Z. Xingguo, H. Hai, J. Junze, Microstructures and mechanical characteristics of electromagnetic casting and direct-chill casting 2024 aluminum alloys, Materials Science and Engineering A 327 (2) (2002) 133–137. doi:10.1016/S0921-5093(01)01673-2.

[11] H. Z. Fu, J. Shen, L. Liu, Q. T. Hao, S. M. Li, J. S. Li, Electromagnetic shaping and solidification control of Ni-base superalloys under vacuum, Journal of Materials Processing Technology 148 (1) (2004) 25–29. doi:10.1016/j.jmatprotec.2003.11.039.

[12] J. D. Jackson, Classical electrodynamics, 3rd Edition, Wiley, 1998.

[13] J.-P. Brancher, O. E. Séro-Guillaume, Étude de la déformation d'un liquide magnétique, Archive for Rational Mechanics and Analysis 90 (1) (1985) 57–85. doi:10.1007/BF00281587.

[14] A. Gagnoud, J. Etay, M. Garnier, Le problème de frontière libre en lévitation électromagnétique, Journal de Mécanique Théorique et Appliquée 5 (6) (1986) 911–934.

[15] A. Henrot, M. Pierre, Un problème inverse en formage des métaux liquides, RAIRO Modélisation Mathématique et Analyse Numérique 23 (1) (1989) 155–177.

[16] H. K. Moffatt, Magnetostatic equilibria and analogous Euler flows of arbitrarily complex topology. Part 1. Fundamentals, Journal of Fluid Mechanics 159 (1985) 359–378. doi:10.1017/S0022112085003251.

[17] A. Novruzi, J. R. Roche, Second order derivatives, Newton method, application to shape optimization, Tech. Rep. RR-2555, INRIA (1995).

[18] M. Pierre, J. R. Roche, Computation of free surfaces in the electromagnetic shaping of liquid metals by optimization algorithms, European Journal of Mechanics. B Fluids 10 (5) (1991) 489–500.

[19] J. A. Shercliff, Magnetic shaping of molten metal columns, Proceedings of the Royal Society of London. Series A, Mathematical and Physical Sciences 375 (1763) (1981) 455–473. doi:10.1098/rspa.1981.0063.

[20] J.-C. Nédélec, Acoustic and Electromagnetic Equations. Integral Representations for Harmonic Problems, Vol. 144 of Applied Mathematical Sciences, Springer-Verlag, New York, 2001.

[21] K. E. Atkinson, The numerical solution of integral equations of the second kind, Vol. 4 of Cambridge Monographs on Applied and Computational Mathematics, Cambridge University Press, Cambridge, 1997. doi:10.1017/CBO9780511626340.
[22] M. Pierre, J. R. Roche, Numerical simulation of tridimensional electromagnetic shaping of liquid metals, Numerische Mathematik 65 (1) (1993) 203–217. doi:10.1007/BF01385748.
[23] J. R. Roche, Gradient of the discretized energy method and discretized continuous gradient in electromagnetic shaping simulation, Applied Mathematics and Computer Science 7 (3) (1997) 545–565.
[24] J. R. Roche, Adaptive Newton-like method for shape optimization, Control and Cybernetics 34 (1) (2005) 363–377.
[25] A. Novruzi, J. R. Roche, Newton's method in shape optimisation: A three-dimensional case, BIT. Numerical Mathematics 40 (1) (2000) 102–120. doi:10.1023/A:1022370419231.
[26] T. P. Felici, J.-P. Brancher, The inverse shaping problem, European Journal of Mechanics. B Fluids 10 (5) (1991) 501–512.
[27] G. Hsiao, W. L. Wendland, Boundary Integral Equations, Vol. 164 of Applied Mathematical Sciences, Springer-Verlag, Berlin, 2008.
[28] J. Giroire, Formulation variationnelle par équations intégrales de problèmes aux limites extérieurs, Tech. Rep. 6, Centre de Mathématiques Appliquées de l'Ecole Polytech-nique (1976).
[29] H. Eschenauer, V. Kobelev, A. Schumacher, Bubble method for topology and shape optmization of structures, Structural Optimization 8 (1) (1994) 42–51.
[30] J. Sokołowski, A. Żochowski, On the topological derivative in shape optimization, SIAM Journal on Control and Optimization 37 (4) (1999) 1251–1272. doi:10.1137/S0363012997323230.
[31] J. Céa, S. Garreau, P. Guillaume, M. Masmoudi, The shape and topological optimizations connection, Computer Methods in Applied Mechanics and Engineering 188 (4) (2000) 713–726.
[32] S. Amstutz, S. M. Giusti, A. A. Novotny, E. A. de Souza Neto, Topological derivative in multi-scale linear elasticity models applied to the synthesis of microstructures, International Journal for Numerical Methods in Engineering 84 (6) (2010) 733–756. doi:10.1002/nme.2922.
[33] S. Amstutz, A. A. Novotny, Topological optimization of structures subject to von Mises stress constraints, Structural and Multidisciplinary Optimization 41 (3) (2010) 407–420. doi:10.1007/s00158-009-0425-x.
[34] A. A. Novotny, R. A. Feijóo, E. Taroco, C. Padra, Topological sensitivity analysis for three-dimensional linear elasticity problem, Computer Methods in Applied Mechanics and Engineering 196 (41-44) (2007) 4354–4364. doi:10.1016/j.cma.2007.05.006.
[35] S. Amstutz, I. Horchani, M. Masmoudi, Crack detection by the topological gradient method, Control and Cybernetics 34 (1) (2005) 81–101.
[36] G. R. Feijóo, A new method in inverse scattering based on the topological derivative, Inverse Problems 20 (6) (2004) 1819–1840. doi:10.1088/0266-5611/20/6/008.
[37] B. B. Guzina, M. Bonnet, Small-inclusion asymptotic of misfit functionals for inverse problems in acoustics, Inverse Problems 22 (5) (2006) 1761–1785. doi:10.1088/0266-5611/22/5/014.
[38] M. Hintermüller, A. Laurain, Electrical impedance tomography: from topology to shape, Control and Cybernetics 37 (4) (2008) 913–933.
[39] M. Hintermüller, A. Laurain, A. A. Novotny, Second-order topological expansion for electrical impedance tomography, Advances in Computational Mathematics 36 (2) (2012) 235–265. doi:10.1007/s10444-011-9205-4.
[40] L. J. Belaid, M. Jaoua, M. Masmoudi, L. Siala, Application of the topological gradient to image restoration and edge detection, Engineering Analysis with Boundary Elements 32 (11) (2008) 891–899. doi:10.1016/j.enganabound.2008.01.004.
[41] M. Hintermüller, A. Laurain, Multiphase image segmentation and modulation recovery based on shape and topological sensitivity, Journal of Mathematical Imaging and Vision 35 (2009) 1–22. doi:10.1007/s10851-009-0150-5.
[42] I. Larrabide, R. A. Feijóo, A. A. Novotny, E. Taroco, Topological derivative: a tool for image processing, Computers & Structures 86 (13-14) (2008) 1386–1403. doi:10.1016/j.compstruc.2007.05.004.
[43] A. A. Novotny, J. Sokołowski, Topological derivatives in shape optimization, Interaction of Mechanics and Mathematics, Springer, 2013.
[44] S. Amstutz, Sensitivity analysis with respect to a local perturbation of the material property, Asymptotic Analysis 49 (1-2) (2006) 87–108.
[45] J. R. de Faria, A. A. Novotny, On the second order topologial asymptotic expansion, Structural and Multidisciplinary Optimization 39 (6) (2009) 547–555. doi:10.1007/s00158-009-0436-7.
[46] S. Garreau, P. Guillaume, M. Masmoudi, The topological asymptotic for PDE systems: the elasticity case, SIAM Journal on Control and Optimization 39 (6) (2001) 1756–1778. doi:10.1137/S0363012900369538.
[47] S. A. Nazarov, J. Sokołowski, Asymptotic analysis of shape functionals, Journal de Mathématiques Pures et Appliquées 82 (2) (2003) 125–196. doi:10.1016/S0021-7824(03)00004-7.
[48] J. Sokołowski, A. Żochowski, Optimality conditions for simultaneous topology and shape optimization, SIAM Journal on Control and Optimization 42 (4) (2003) 1198–1221. doi:10.1137/S0363012901384430.
[49] H. Ammari, H. Kang, Reconstruction of small inhomogeneities from boundary measurements, Lectures Notes in Mathematics vol. 1846, Springer-Verlag, Berlin, 2004.

[50] H. Ammari, H. Kang, Polarization and moment tensors with applications to inverse problems and effective medium theory, Applied Mathematical Sciences vol. 162, Springer-Verlag, New York, 2007.
[51] D. Sarason, Complex function theory, 2nd Edition, American Mathematical Society, Providence, RI, 2007.
[52] S. Osher, J. Sethian, Front propagating with curvature dependent speed: algorithms based on hamilton-jacobi formulations, Journal of Computational Physics 78 (1988) 12–49. doi:10.1016/0021-9991(88)90002-2.

(A. Canelas) Instituto de Estructuras y Transporte, Facultad de Ingeniería, Universidad de la República, J. Herrera y Reissig 565, CP 11300, Montevideo, Uruguay
E-mail address: acanelas@fing.edu.uy

(A.A. Novotny) Laboratório Nacional de Computação Científica LNCC/MCT, Av. Getúlio Vargas 333, 25651-075, Petrópolis – RJ, Brazil
E-mail address: novotny@lncc.br

(J.R. Roche) Institut Elie Cartan de Lorraine, Université de Lorraine, CNRS, INRIA, B.P. 70239, 54506, Vandoeuvre lès Nancy, France
E-mail address: roche@iecn.u-nancy.fr